

# RSC Advances



This is an *Accepted Manuscript*, which has been through the Royal Society of Chemistry peer review process and has been accepted for publication.

*Accepted Manuscripts* are published online shortly after acceptance, before technical editing, formatting and proof reading. Using this free service, authors can make their results available to the community, in citable form, before we publish the edited article. This *Accepted Manuscript* will be replaced by the edited, formatted and paginated article as soon as this is available.

You can find more information about *Accepted Manuscripts* in the [Information for Authors](#).

Please note that technical editing may introduce minor changes to the text and/or graphics, which may alter content. The journal's standard [Terms & Conditions](#) and the [Ethical guidelines](#) still apply. In no event shall the Royal Society of Chemistry be held responsible for any errors or omissions in this *Accepted Manuscript* or any consequences arising from the use of any information it contains.

# Photothermal and Photodynamic Therapy Reagents based on rGO-C<sub>6</sub>H<sub>4</sub>-COOH

Guangcheng Wei, Miaomiao Yan, Liying Ma, Chunhua Wang\*

The Key Laboratory of Traditional Chinese Medicine Prescription Effect and Clinical Evaluation  
of State Administration of Traditional Chinese Medicine

Binzhou Medical College, Department of pharmacy science, 264003, Yantai, China

[\*] Prof. C. Wang is the corresponding author. E-mail: Chhuawang@126.com

## Abstract:

A photothermal therapy (PTT) and photodynamic therapy (PDT) reagent was synthesized based on the rGO-C<sub>6</sub>H<sub>4</sub>-COOH (graphene diazotized). The rGO-C<sub>6</sub>H<sub>4</sub>-COOH was firstly conjugated with polyethyleneimine (PEI) to enhance the water solubility, and then the tetrakis (4-carboxyphenyl) porphyrin (TCPP) was further attached with the system to obtain the ability of PDT. The rGO-PEI-TCPP system exhibited excellent stability in various biological solutions and the cytotoxicity of rGO-PEI-TCPP system was acceptable. The CBRH7919 cancer cell could be induced effectively apoptosis by the rGO-PEI-TCPP under laser irradiation. The reason attributed to mainly the excellent photothermal and photodynamic effect, that is to say, the production of heat and singlet oxygen. At the same time, the CBRH7919 cancer cell could be pushed to the vulnerable G2 phase of the cell cycle, which is the most sensitive and susceptible to damage by radiation.

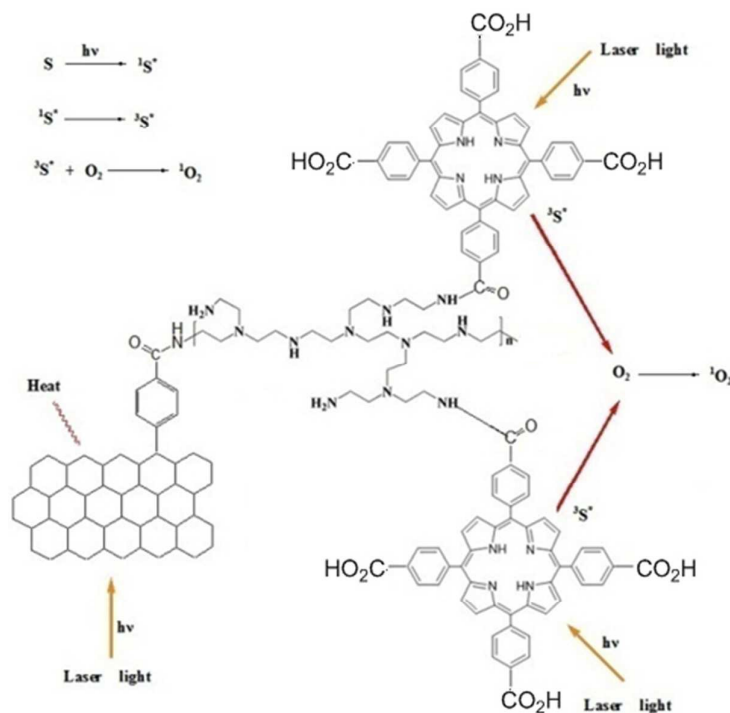
**Key words:** graphene, photothermal therapy, photodynamic therapy, porphyrin, apoptosis

## 1. Introduction

Graphene has been applied widely to the field of nano-electronic devices<sup>1,2</sup>, transparent conductors<sup>3,4</sup>, and nanocomposites<sup>5</sup> in the past few years. A new direction for graphene is in the field of photothermal therapy (PTT) and photodynamic therapy (PDT), and PTT based on graphene have been completely designed from graphene oxide (GO) and reduced graphene oxide (rGO), as the degree of conjugation of planar GO is negligible<sup>6-22</sup>. So the effect of PTT would be not ideal. The rGO colloidal solution has a tendency to agglomerate irreversibly in the absence of stabilizer, thus making further processing difficult<sup>23</sup>. Photodynamic therapy (PDT) is a minimally

invasive therapeutic modality approved for the treatment of cancer diseases and non-oncological disorders. Extensive studies on the synthesis of various porphyrin derivatives have been reported<sup>15, 16, 23</sup>. Photoirradiation with a specific wavelength to the porphyrin derivatives induces reactions generating radicals such as hydroxyl (OH) and peroxy (HO<sub>2</sub>) radicals, as well as non-radical, and highly reactive singlet oxygen (<sup>1</sup>O<sub>2</sub>). The main cytotoxicity agent in PDT is widely believed to be <sup>1</sup>O<sub>2</sub>, and direct and indirect evidence supports a prevalent role for <sup>1</sup>O<sub>2</sub> in the molecular processes initiated by PDT<sup>24, 25</sup>.

Herein, rGO-PEI-TCPP (rGO-C<sub>6</sub>H<sub>4</sub>-CO-NH-PEI-NH-OC-TCPP) system was synthesized. According to our previous research<sup>26</sup>, the conjugation degree of rGO-C<sub>6</sub>H<sub>4</sub>-COOH is higher than GO. So the effect of PTT should be better than GO, and at the same time the TCPP molecular could be used as the PDT. A schematic representation was shown in scheme 1.



Scheme 1. PTT and PDT illustration drawing of rGO-PEI-TCPP system.

## 2. Experimental:

### 2.1 Synthesis of graphene oxide (GO), reduced graphene oxide (rGO) and rGO-C<sub>6</sub>H<sub>4</sub>-COOH:

GO, rGO and rGO-C<sub>6</sub>H<sub>4</sub>-COOH were synthesized according to our previous method, and the detailed synthesis process could be seen in the supporting information<sup>26</sup>. Solid samples of rGO and rGO-C<sub>6</sub>H<sub>4</sub>-COOH were obtained through freeze-drying for the FT-IR characterization. The

solutions of GO, rGO and rGO-C<sub>6</sub>H<sub>4</sub>-COOH were put on a thin film of amorphous carbon deposited on a copper grid for TEM (JEM-1400) observation. One drop of rGO-C<sub>6</sub>H<sub>4</sub>-COOH solution was dropped onto the silicon wafer for the AFM (Nanoscope IIIA, Veeco) images. The colloidal nature of rGO and rGO-C<sub>6</sub>H<sub>4</sub>-COOH dispersion solutions was demonstrated by the Tyndall effect which suggests excellent water dispersibility.

## 2.2 Synthesis of rGO-C<sub>6</sub>H<sub>4</sub>-CO-NH-PEI and rGO-C<sub>6</sub>H<sub>4</sub>-TCPP

The rGO-C<sub>6</sub>H<sub>4</sub>-CO-NH-PEI was synthesized by means of 1-ethyl-3-(3-dimethylaminopropyl) carbodiimide (EDC) chemistry. In detail, branched polyethyleneimine (PEI; 1.2 g, M<sub>r</sub> = 1.8 kDa, Alfa Aesar) was dissolved in water (10 mL) under stirring. Then EDC·HCl (0.2 g) and N-hydroxysuccinimide (NHS; 0.15 g) were added to 60 mL aqueous solution of rGO-C<sub>6</sub>H<sub>4</sub>-COOH (The above rGO-C<sub>6</sub>H<sub>4</sub>-COOH solution without further treatment) with stirring for 3 h (pH 5.5–6). Finally, the above two solutions were mixed and stirred for 48 h, and then sonicated for 48 h by using a 500 W sonicator. The mixture was dialyzed (molecular weight cutoff (MWCO): 7000 Da) against water for another 48 h, then centrifuged at 10000 rpm for 10 min to remove any precipitates. A solid sample was obtained by lyophilized freeze-drying for FT-IR spectroscopy.

To conjugate TCPP to rGO-C<sub>6</sub>H<sub>4</sub>-CO-NH-PEI, TCPP was first activated by NHS. In detail, TCPP (2 mmol) was dissolved in anhydrous ethanol (20 mL). NHS (4mmol) and dicyclohexylcarbodiimide (DCC, 4 mmol) were added. The mixture was stirred overnight at room temperature. Filtration was carried out to remove any precipitates. The mixture was mixed with the above aqueous solution of rGO-C<sub>6</sub>H<sub>4</sub>-CO-NH-PEI to produce rGO-PEI-TCPP (Scheme 1) solution with stirring for 48 h. The mixture was then dialyzed against ethanol (MWCO: 3500 Da) for 48 h to remove TCPP, and finally dialyzed against water for another 48 h. The rGO-PEI-TCPP solution was sonicated for 72 h by using a 500 W sonicator to obtain a small-sized product. The solution was used directly for the determination of UV/Vis and fluorescent spectroscopy measurements. One drop of this rGO-PEI-TCPP solution was mounted on a thin film of amorphous carbon deposited on a copper grid for TEM imaging.

## 2.3 Cell lines and cell culture

Mouse liver cancer CBRH7919 cell (cancer cell) were maintained in Dulbecco's Modified Eagle's Medium (DMEM, Fanbo) supplemented with 10% (v/v) fetal bovine serum (FBS, Fanbo), penicillin–streptomycin (1.0% penicillin–streptomycin, 1.0% Glutamax, respectively, Fanbo) in an

incubator supplied with 85% humidity and 5% CO<sub>2</sub> atmosphere at 37°C. The cell culture medium was changed every two days and the cells were split upon 80% confluence.

#### **2.4 Cancer cell uptake**

For cellular uptake, mouse liver cancer CBRH7919 cell (cancer cell) (200 μL, ≈1 million mL<sup>-1</sup>) was incubated with rGO-PEI-TCPP (50 μL) in PBS for 1 h at 37°C. The rGO-PEI-TCPP concentration in the solution during incubation was approximately 1 mg mL<sup>-1</sup>. Cells were washed three times with PBS to remove unbound rGO-PEI-TCPP before confocal fluorescence imaging. The internalized rGO-PEI-TCPP was visually observed by confocal laser scanning microscopy (Leica TCS SPE) on the cover glass.

#### **2.5 Cytotoxicity**

##### **Cck8 assay**

For cck8 assays, cancer cells were seeded into 96-well plates at a density of  $1 \times 10^4$  per well in medium (200 μL). The cells were then incubated with various concentrations of rGO-PEI-TCPP for 48 h. Afterwards, 20 μL cck8 was added to each well, and then were incubated for 1 h. The optical densities were measured at 450nm by using a multidetection microplate reader (Synergy<sup>TM</sup> HT, BioTek Instruments Inc, USA). Data from cck8 assays were analyzed using Origin Pro8.SR3 software and SPSS Statistics V17 software; the significant level was set as  $P < 0.05$ .

##### **FCM assays**

**For FCM assays** using 12-well culture plates, exponentially growing cancer cells were seeded ( $1 \times 10^5$  cell per well) and pre-incubated for 24 h, followed by co-incubation with different concentrations of rGO-PEI-TCPP for 4 8 h. Then the medium was discarded, and the cells were washed three times with PBS. Cells were then detached by trypsinization, centrifuged, and dispersed again in PBS for measurements. Liver cells treated with rGO-PEI-TCPP were stained with propidium iodide (PI) and Annexin V-EGFP before flow cytometry (Coulter Epics XL, America) analysis.

#### **2.6 PTT and PDT**

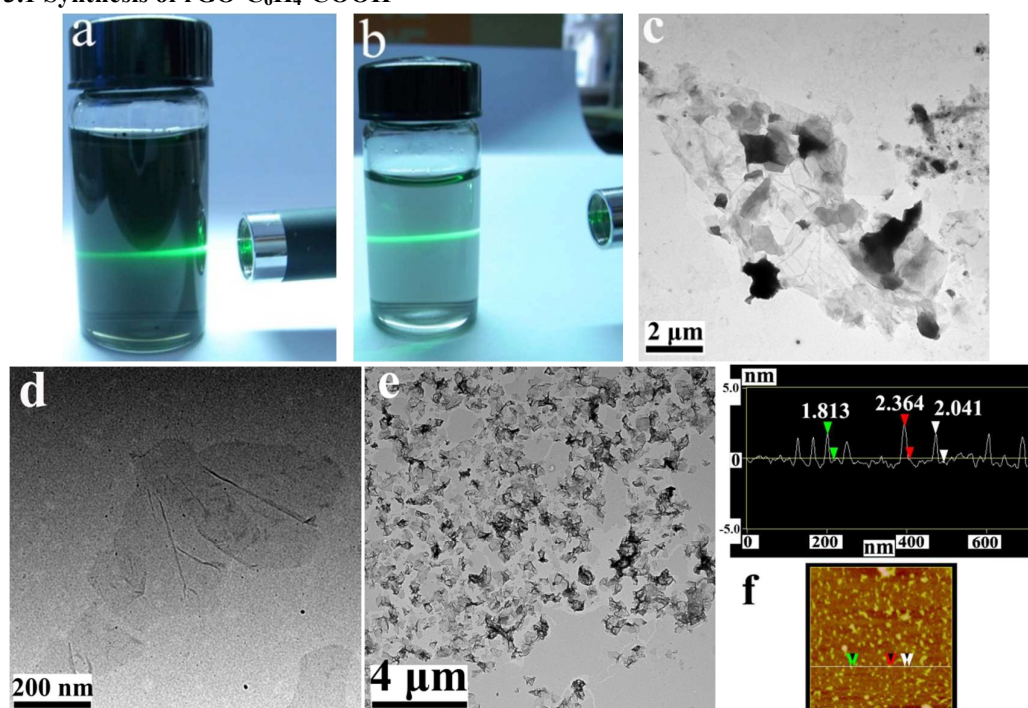
After 1 h of incubation at 37°C with rGO-PEI-TCPP, the cell culture bottle containing cancer cell was stored in carbon dioxide cell incubator until irradiation. The source of irradiation was a 20W 410 nm diode laser (RPMC lasers). Each cancer cell sample was irradiated with the 410 nm laser at a power of 20W after incubations including control cells without any exposure to

rGO-PEI-TCPP. Immediately after heating, cells were seeded in a 96-well plate with 100  $\mu\text{L}$  of media. After 24 h of incubation at 37°C, cell viability and cell-cycle assay was determined by FCM assay.

**Statistical analysis:** Statistical analysis of the data was carried out using Student's t-test, and the analysis was performed using SPSS Statistics V17. Differences were considered statistically significant when the P value was less than 0.05. The data are presented as the mean-standard deviation.

### 3. Result and Discussion

#### 3.1 Synthesis of rGO-C<sub>6</sub>H<sub>4</sub>-COOH



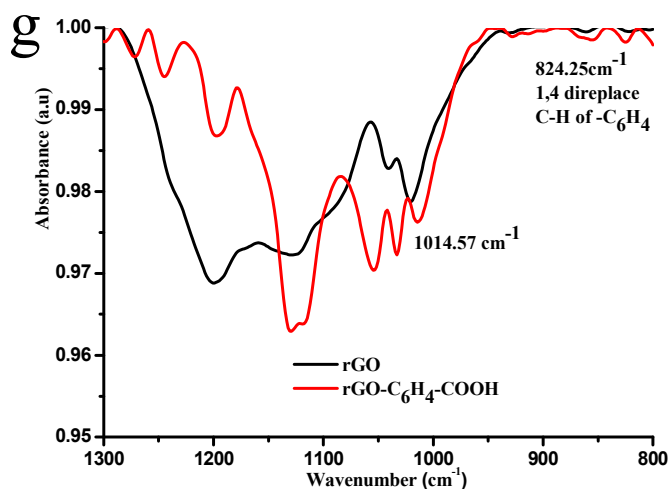


**Figure 1.** Characterization of GO, rGO and rGO-C<sub>6</sub>H<sub>4</sub>-COOH. (a) Tyndall effect of rGO colloidal solution; (b) Tyndall effect of rGO-C<sub>6</sub>H<sub>4</sub>-COOH colloidal solution; (c) TEM image of GO; (d) TEM image of rGO; (e) TEM image of rGO-C<sub>6</sub>H<sub>4</sub>-COOH; (f) AFM image of rGO-C<sub>6</sub>H<sub>4</sub>-COOH; (g) FT-IR spectra of rGO and rGO-C<sub>6</sub>H<sub>4</sub>-COOH.

The Tyndall effect proves the colloidal nature, and the very obvious Tyndall effect of the rGO and rGO-C<sub>6</sub>H<sub>4</sub>-COOH solutions was demonstrated, which were shown in figure 1a and figure 1b, suggesting that these solutions have excellent dispersibility in aqueous solution. TEM observations were performed to demonstrate the morphologies of GO, rGO and rGO-C<sub>6</sub>H<sub>4</sub>-COOH. One can see that the GO (Figure 1c) has a continuous big sheet, and rGO sheets have the ripple lines between the layers, which were demonstrated in figure 1d, suggesting high quality rGO sheets were prepared. As was shown in figure 1e, the rGO-C<sub>6</sub>H<sub>4</sub>-COOH sheets are very seriously accumulated between the graphene layers, and when the rGO-C<sub>6</sub>H<sub>4</sub>-COOH is in a solid state, the fold on the edge can also be found. The conjugation of the p-disubstituted phenyl group (-C<sub>6</sub>H<sub>4</sub>-COOH) with the planar rGO was confirmed by AFM observations and FT-IR measurements. The height of the rGO-C<sub>6</sub>H<sub>4</sub>-COOH sheets was confirmed by the AFM observations, which was shown in figure 1f. The height mostly lies in the range from 1.6–3.2 nm. The theoretical height of the single-layer rGO-C<sub>6</sub>H<sub>4</sub>-R (R = COOH, NO<sub>2</sub>, OCH<sub>3</sub>, or Br) sheet on both sides is about 2.2 nm, and the height of the bare rGO sheets is about 1.0 nm with the substituted aromatic groups contributing about 0.6 nm in height<sup>27</sup>. The height ranging from 1.6 nm to 3.2 nm suggests that single-layer and double-layer of rGO-C<sub>6</sub>H<sub>4</sub>-COOH coexist, and the -C<sub>6</sub>H<sub>4</sub>-COOH groups were attached and perpendicularly standing to one side, as well as both

sides of the rGO sheets. The p-disubstituted phenyl group ( $-\text{C}_6\text{H}_4-\text{COOH}$ ) of  $\text{rGO}-\text{C}_6\text{H}_4-\text{COOH}$  was confirmed by FT-IR measurements, as was shown in Figure 1g, The peak at  $1014.57\text{ cm}^{-1}$  is the characteristic vibration of the p-disubstituted phenyl group, and the peak at  $824.25\text{ cm}^{-1}$  is the C–H bending vibration of the p-disubstituted phenyl group.<sup>28,29</sup>

### 3.2 Synthesis of rGO-PEI-TCPP

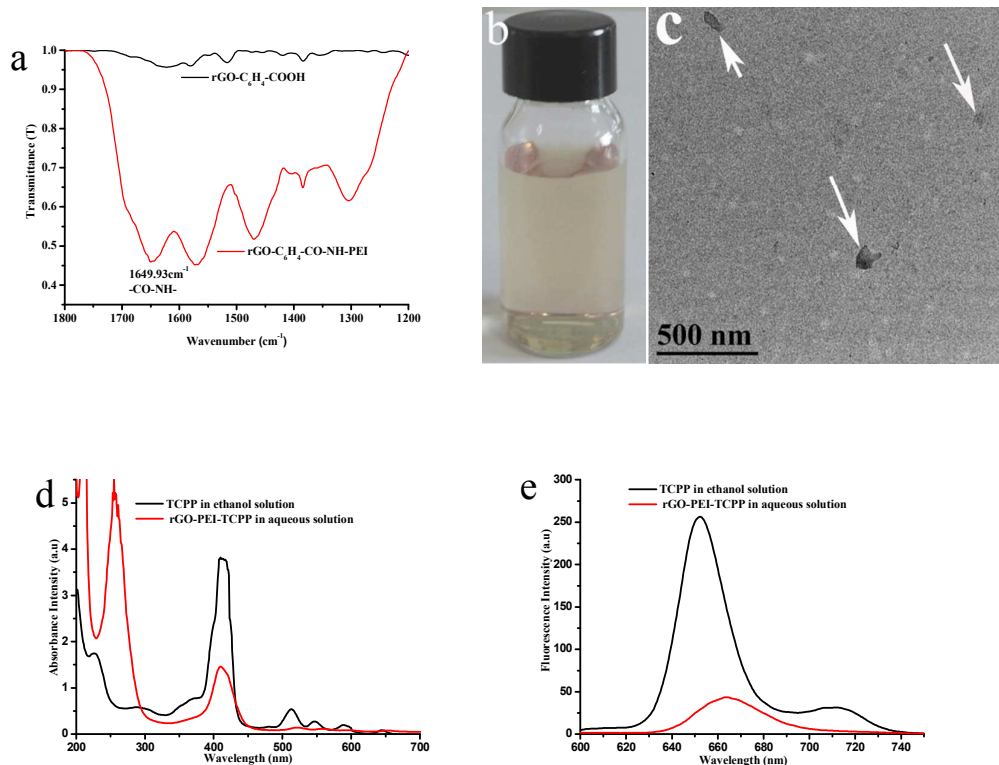


**Figure 2.** Characterization of  $\text{rGO}-\text{C}_6\text{H}_4-\text{CO}-\text{NH}-\text{PEI}$  and  $\text{rGO}-\text{PEI}-\text{TCPP}$ . (a) FT-IR spectra of  $\text{rGO}-\text{C}_6\text{H}_4-\text{COOH}$  and  $\text{rGO}-\text{C}_6\text{H}_4-\text{CO}-\text{NH}-\text{PEI}$ ; (b)  $\text{rGO}-\text{PEI}-\text{TCPP}$  colloidal solution; (c) TEM image of  $\text{rGO}-\text{PEI}-\text{TCPP}$ ; (d) UV visible spectra of TCPP and  $\text{rGO}-\text{PEI}-\text{TCPP}$ ; (e) Fluorescence spectra of TCPP and  $\text{rGO}-\text{PEI}-\text{TCPP}$ .

According to the comparison of the FT-IR spectra of  $\text{rGO}-\text{C}_6\text{H}_4-\text{CO}-\text{NH}-\text{PEI}$  with  $\text{rGO}-\text{C}_6\text{H}_4-\text{COOH}$  (Figure 2a), a characteristic amide–carbonyl (C=O vibration of NH- CO group) stretching vibration at approximately  $1649.93\text{ cm}^{-1}$ <sup>30</sup> is consistent with the branched PEI molecules on  $\text{rGO}-\text{C}_6\text{H}_4-\text{COOH}$  sheets. The appearance of this characteristic peaks revealed the successful conjugation of the  $-\text{COOH}$  ( $\text{rGO}-\text{C}_6\text{H}_4-\text{COOH}$ ) group with the  $-\text{NH}_2$  (PEI) group. Figure 2b is the colloidal solution of  $\text{rGO}-\text{PEI}-\text{TCPP}$ , and the TEM image in figure 2c (The sheet of  $\text{rGO}-\text{PEI}-\text{TCPP}$  were marked by white arrows) showed that the size of  $\text{rGO}-\text{PEI}-\text{TCPP}$  was about 20-50 nm. Because of the difficulty in confirming the conjugation of  $\text{rGO}-\text{C}_6\text{H}_4-\text{CO}-\text{NH}-\text{PEI}$  with TCPP by means of FT-IR spectra, UV/Vis spectra were used to

analyze the conjugation. By comparing the UV/Vis spectra (Figure 2d) of TCPP in ethanol solution with rGO-PEI-TCPP in aqueous solution, one can see that the peak overlap of two compounds, which indicates that TCPP was conjugated to rGO-C<sub>6</sub>H<sub>4</sub>-CO-NH-PEI,<sup>31</sup> and the fluorescence spectra support this point also (Figure 2e). The rGO-PEI-TCPP colloidal solution was very stable and could exist in various kinds of biological solution without aggregation (Figure S1).

### 3.3 Cytotoxicity of rGO-PEI-TCPP

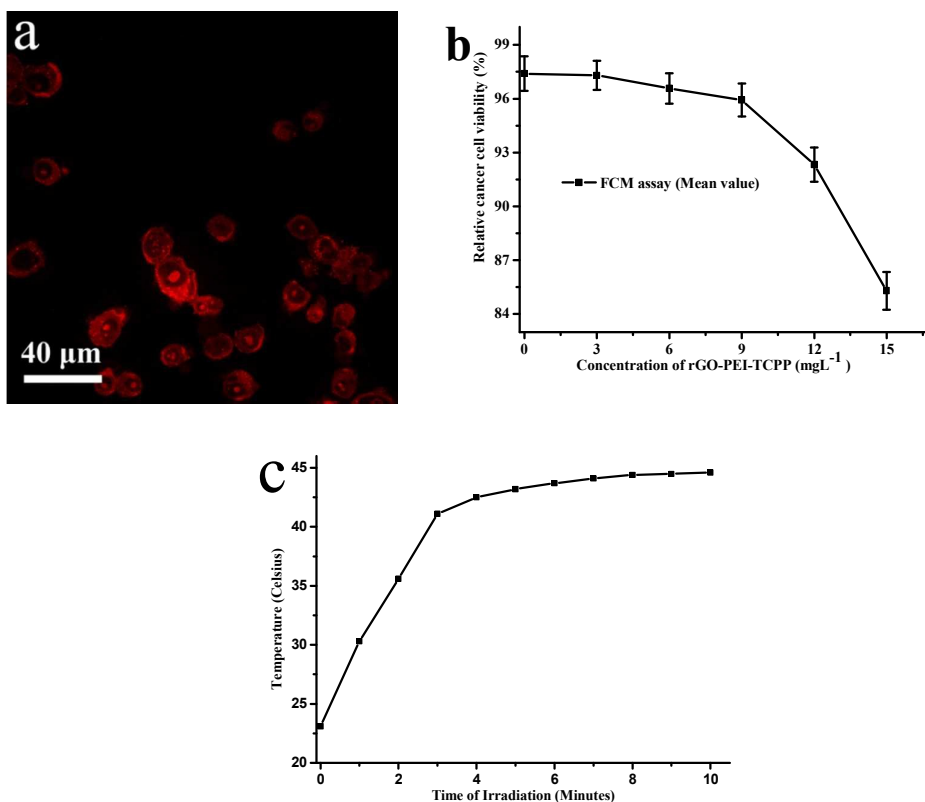


**Figure 3.** (a) Confocal laser fluorescence images of rGO-PEI-TCPP which was uptake by CBRH7919 cancer cells,  $\lambda_{ex}$ =532 nm, darkness field; b) The effect of rGO-PEI-TCPP concentration to relative CBRH7919 cancer cell viability; c) Temperature change curves of the CBRH7919 cancer cell solution which was treated with rGO-PEI-TCPP with the irradiation time increasing.

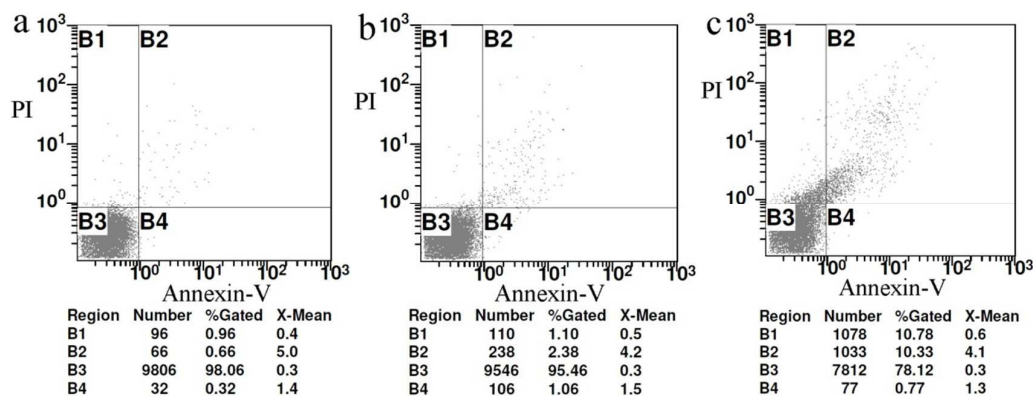
Group	Concentration/mg·L <sup>-1</sup>	24 h (%)	48 h (%)	72 h (%)
Control	0	102.9±3.2	94.1±5.5	93.3±4.3
rGO-PEI-TCPP	3	97.5±1.8	93.8±3.1 <sup>△</sup>	91.6±2.6 <sup>△</sup>
rGO-PEI-TCPP	6	97.3±1.8	91.9±3.2 <sup>△</sup>	91.4±3.1

rGO- PEI-TCPP	9	93.1±0.9 <sup>△</sup>	91.6±1.5 <sup>△</sup>	89.8±1.1 <sup>△</sup>
rGO- PEI-TCPP	12	91.6±2.0 <sup>△</sup>	88.8±3.5 <sup>△</sup>	85.2±2.8 <sup>△</sup>
rGO- PEI-TCPP	15	89.8±1.5 <sup>△</sup>	88.1±1.9	84.9±2.5 <sup>△</sup>

**Table1.** Cck8 assay: Effect of different concentrations of rGO-PEI-TCPP for cancer cell viability ( $\% \pm s$ ,  $\Delta$  behalf of  $P < 0.05$ )

The uptake behavior of rGO-PEI-TCPP by cancer cells was demonstrated with the confocal laser fluorescence microscopy imaging (Figure 3a). The cytotoxicity of rGO-PEI-TCPP was determined by using FCM (Flow cytometer) assay (Figure 3b and figure S2) and cck8 assay (Table 1) with CBRH7919 cells. In the cck8 assay (Table 1), the rGO-PEI-TCPP has no obvious toxicity to CBRH7919 cells at the concentrations of up to 15 mg mL<sup>-1</sup>, meaning that the relative cancer cell viability is not less than 80%. The result of the FCM assay is very similar with that of the cck8 assay, as was shown in Figure 3b. According to the results of the cck8 assay and FCM assay, the rGO-PEI-TCPP concentration of 10 mg mL<sup>-1</sup> was used for the PTT and PDT in the current experiment. Under irradiation, the temperature of the cell pellets increased in the first minute of irradiation and then leveled off at ~44 °C for CBRH7919 cancer cell treated with rGO-PEI-TCPP (Figure 3c). After replating the cells in a 96-well plate (n = 6) along with the cells not exposed to 410 nm irradiation, we monitored cell viability after 24 h. CBRH7919 cancer cells incubated with rGO-PEI-TCPP and irradiated with 410 nm visible light for 5 min before FCM apoptosis assay and cell cycle assay after 24h.

### 3.4 Apoptosis and cell cycle life



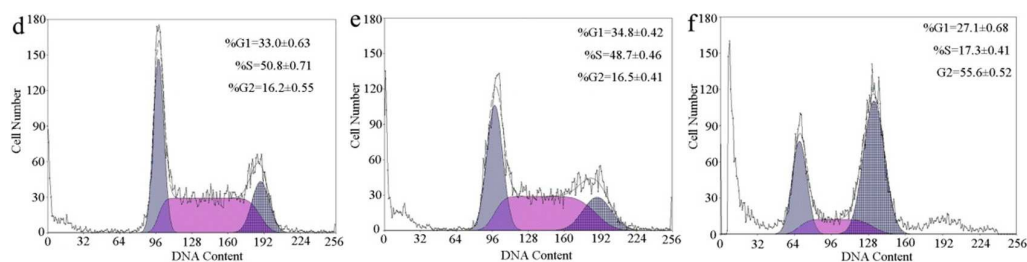


**Figure 4.** Effect of rGO-PEI-TCPP on apoptosis and cell cycle of CBRH-7919 cell line. (a) Control apoptosis group; (b)  $10 \text{ mg}\cdot\text{L}^{-1}$  rGO-PEI-TCPP apoptosis group without irradiated; (c)  $10 \text{ mg}\cdot\text{L}^{-1}$  rGO-PEI-TCPP apoptosis group irradiated; (d) Control cell cycle group; (e)  $10 \text{ mg}\cdot\text{L}^{-1}$  rGO-PEI-TCPP cell cycle group without irradiated; (f)  $10 \text{ mg}\cdot\text{L}^{-1}$  rGO-PEI-TCPP cell cycle group irradiated. In the FCM figures (a, b, c), B1, B2, B3 and B4 zone denote the cell necrosis period, the late apoptotic cells period, the normal cell death period and the early apoptotic cells period separately.

The effect of rGO-PEI-TCPP as PTT and PDT reagent to induce CBRH7919 cancer cell apoptosis can be analyzed with FCM (Figure 4a, b, c and figure S3, S4, S5). The cancer cell viability of the control group is about 98.06 % (Figure 4a), and the  $10 \text{ mg L}^{-1}$  rGO-PEI-TCPP group without radiation is about 95.46% (Figure 4b), which indicates the low toxicity. However the cancer cell viability of untreated cancer cells by rGO-PEI-TCPP ( $10 \text{ mg L}^{-1}$ ) with the laser irradiation is about 92.59% (Figure S3b), comparing with the control group (Figure S3a), which shows the laser irradiation can induce the cancer cell slightly apoptosis. With the same concentration of rGO-PEI-TCPP ( $10 \text{ mg L}^{-1}$ ) with irradiation, the viability of cancer cell irradiated decreased sharply. It is about 78.12%, that is to say, the rGO-PEI-TCPP as the reagent of PTT and PDT could effectively induce the cancer cell apoptosis. It could be further proved by the confocal laser fluorescence microscopy imaging (Figure S4), and comparing with the control group (Figure S4a, b), the morphology of cancer cell in  $10 \text{ mg}\cdot\text{L}^{-1}$  rGO-PEI-TCPP group without irradiation had almost no change (Figure S4c, d), which indicated the low cytotoxicity. However, the  $10 \text{ mg}\cdot\text{L}^{-1}$  rGO-PEI-TCPP group with irradiations could cause to the cancer cell morphology deformation (Figure S4e, f), and the cancer cell shape was apparently contractible, most of which turned rounded and condensation. At the same time, spherical protrusions at the cell surface and apoptotic bodies was observed, which was the classic character of apoptosis. Meanwhile, as another control experiment (Figure S5), the rGO- $\text{C}_6\text{H}_4\text{-CO-NH-PEI}$  could also induce the cancer cell apoptosis with the irradiation, and the cell viability is about 87.75% (Figure S5c), comparing to the control group (Figure S5a) and without irradiation group (Figure S5b), the apoptosis effect of rGO- $\text{C}_6\text{H}_4\text{-CO-NH-PEI}$  was less than rGO-PEI-TCPP (Figure 4c). The reason mainly included

mainly two aspects, one is the existence of graphene group. When the laser irradiated the plane of graphene, the heat would be produced, and the temperature of solution would increase, which could induced the cancer cell apoptosis<sup>6,8</sup>; The other one is the existence of porphyrin group, according to reference, the singlet oxygen would be produced when the laser radiated the mixture solution, and the singlet oxygen is very effectively germicide, and it could effectively kill the cancer cell<sup>24,25</sup>.

In a cell population, the effect of rGO-PEI-TCPP as PTT and PDT reagent on each cell varies as the cell advances through the cell cycle (Figure 4d, e, f). The CBRH7919 cancer cells were employed for the cell cycle assay. As was shown in figure 4d, the CBRH7919 cancer cells of control group in the cell cycle assay tend to block in the S phase, i.e.,  $50.8\% \pm 0.71$ ,  $16.2 \pm 0.55\%$  in G2 (G2/M) phase, and  $33.0 \pm 0.63\%$  in G1 phase (G0/G1). Compared with the control group, the  $10 \text{ mgL}^{-1}$  rGO-PEI-TCPP group (Figure 4e) which was not radiated by laser light can induce the CBRH7919 cancer cell block mostly in the S phase ( $48.7\% \pm 0.46\%$ ) and G1 phase ( $34.8 \pm 0.42\%$ ), and the arrested rate of the G1 phase is about  $16.5 \pm 0.41\%$ , which is similar to the control group. This suggests that the rGO-PEI-TCPP is not apoptosis effect at the current concentration ( $10 \text{ mg L}^{-1}$ ) to CBRH7919 cancer cells. As was shown in figure 4f for rGO-PEI-TCPP group which was radiated by laser light, the arresting rate of the G1 phase is  $27.1 \pm 0.68\%$  and the S phase is  $17.3 \pm 0.41\%$ , suggesting that the DNA synthesis of CBRH7919 cell is active after being treated with rGO-PEI-TCPP which was radiated by laser light and the restriction point requirements have been met<sup>32</sup>. However, the G2 phase shows a great difference with the control groups and  $10 \text{ mgL}^{-1}$  rGO-PEI-TCPP group which was not radiated, and the arresting rate is  $55.6 \pm 0.52\%$ , suggesting that the RNA synthesis and the chromatin spiral of CBRH7919 cancer cells treated with rGO-PEI-TCPP which was radiated are active. After 24 h, the concentration of nanomaterials in the cells could be ranked according to the different phases:  $G2/M > S > G0/G1$ , and the cancerous cells can pass through S or G2/M phases more often than healthy cells. The cells are the most sensitive in the late M and G2 phases and most resistant in the late S phase. The pattern of resistance and sensitivity correlates with the level of sulfhydryl compounds in the cells. Sulfhydryls are natural radioprotectors and tend to be at their highest levels in S and at their lowest near mitosis.<sup>33</sup> As shown by rGO-PEI-TCPP group which was radiated in our experiments, it could effectively hinder the CBRH7919 cancer cells in the G2 phase and prevent the

CBRH7919 cancer cells from entering the mitosis period (M phase).

#### 4. Conclusions

Herein, rGO-PEI-TCPP which was a PTT and PDT reagent based on the rGO-C<sub>6</sub>H<sub>4</sub>-COOH (graphene diazotized) was synthesized. The rGO-PEI-TCPP had excellent stability in various biological solutions and low cytotoxicity. The rGO-PEI-TCPP could induce effectively the CBRH7919 cancer cell apoptosis under the laser irradiation through the PTT and PDT function, at the same time, the CBRH7919 cancer cell could be pushed to the vulnerable G2 phase of the cell cycle, which is most sensitive and susceptible to damage by irradiation.

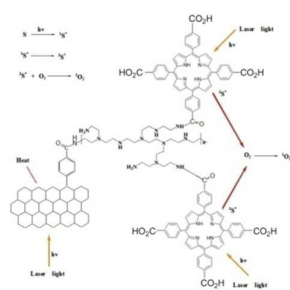
#### 5. Acknowledgements

This work was financially supported by NSFC (Grant No. 21201020), Shandong Provincial Independent Innovation and Achievements Transformation Foundation (Grant No.2014CGZH1316), Shandong Provincial Natural Science Foundation., China (Grant Nos. ZR2013BM022) and a Project of Shandong Province Higher Educational Science and Technology Program (Grant No. J15LC01).

#### Reference

1. L. Jiao, L. Zhang, X. Wang, et al., *Nature* **2009**, 458, 877–880.
2. X. Li; X. Wang, L. Zhang, et al., *Science* **2008**, 319, 1229–1232.
3. X. Li, G. Zhang, X. Bai, et al., *Nat. Nanotech.*, **2008**, 3, 538-542.
4. K. S. Kim, Y. Zhao, H. Jang, et al., *Nature*, **2009**, 457,706– 710.
5. S.D.D.A. Stankovich, G.H.B. Dommett, K.M.Z.E.J. Kohlhaas, et al., *Nature* **2006**, 282–286.
6. K. Yang, S. Zhang, G.X. Zhang, et al., *Nano Lett.* **2010**, 10, 3318–3323.
7. J. F. Lovell, C. S. Jin, E. Huynh, et al., *Nature Materials*. **2011**, 10, 324-332.
8. J. T. Robinson, S. M. Tabakman, Y.Y. Liang, et al., *J. Am. Chem. Soc.* **2011**, 133, 6825–6831.
9. J. F. Lovell, C. S. Jin, E. Huynh, et al., *Angew. Chem. Int. Ed.* **2012**, 51, 2429–2433.
10. E. Huynh, J. F. Lovell, B. L. Helfield, et al., *J. Am. Chem. Soc.* **2012**, 134, 16464–16467.
11. T. Numata, T. Murakami, F. Kawashima, et al., *J. Am. Chem. Soc.* **2012**, 134, 6092–6095.
12. J. L. Li, H.C. Bao, X. L. Hou, et al., *Angew. Chem. Int. Ed.* **2012**, 51, 1830–1834.
13. A. Harada, M. Ono, E. Yuba et al., *Biomater. Sci.*, **2013**, 1, 65–73.
14. R. Bonnett, et al., *Chem. Soc. Rev.*, **1995**, 24, 19-33.
15. E. D. Sternberg, D. Dolphin, C. Brücker, *Tetrahedron*. **1998**, 54, 4154-4202.

16. J. Schmitt, V. Heitz, A. Sour, et al., *Angew. Chem. Int. Ed.* **2015**, 54, 169–173.
17. M. Nurunnabi, K. Parvez, M. Nafiujjaman, et al., *RSC Adv.*, **2015**, 5, 42141–42161.
18. H. D. Chen, F.Y. Liu, Z. Lei, et al., *RSC Adv.*, **2015**, 5, 84980–84987.
19. Z. Hu, J. Li, Y. D. Huang, et al., *RSC Adv.*, **2015**, 5, 654–664.
20. M. J. Hajipour, O. Akhavan, A. Meidanchi, et al., *RSC Adv.*, **2014**, 4, 62557–62565.
21. J. M. Shen, F. Y. Gao, L. P. Guan, et al., *RSC Adv.*, **2014**, 4, 18473–18484.
22. Y.P. Zeng, Z.Y. Yang, S.L. Luo, et al., *RSC Adv.*, **2015**, 5, 57725–57734.
23. P. Laaksonen, A. Walther, J. M. Malho, et al., *Angew. Chem. Int. Ed.* **2011**, 123, 8847–8850.
24. T. Murakami, H. Nakatsuji, M. Inada, et al., *J. Am. Chem. Soc.* **2012**, 134, 17862–17865.
25. A. Harada, M. Ono, E. Yuba, et al., *Biomater. Sci.*, **2013**, 1, 65–73
26. G.C. Wei, M.M Yan, R.H. Dong, et al., *Chem. Eur. J.* **2012**, 18, 14708–14716.
27. J. R. Lomeda, C. D. Doyle, D. V. Kosynkin, et al., *J. Am. Chem. Soc.*, **2008**, 130, 16201–16206.
28. L. Zhang, J. Xia, Q. Zhao, et al., *Small*, **2010**, 6, 537–544.
29. Y. Si and E. T. Samulski, *Nano Lett.*, **2008**, 8, 1679–1682.
30. X. M. Sun, Z. Liu, K. Welsher, et al., *Nano Res.* **2008**, 1, 203–212;
31. L. M. Zhang, J. G. Xia, Q. H. Zhao, et al., *Small* **2010**, 6, 537–544;
32. E. Valk, R. Venta, A. Iofik, et al., *Nature*, **2011**, 480, 128–132.
33. M. Mahmoudi, K. Azadmanesh, M. A. Shokrgozar, et al., *Chem. Rev.*, **2011**, 111, 3407–3432.



A photothermal and photodynamic therapy reagents based on rGO-C<sub>6</sub>H<sub>4</sub>-COOH was developed, and it could induce effectively cancer cell apoptosis.